ELSEVIER

Catalysis Today 26 (1995) 275–282

CATALYSIS TODAY

Modelling channel interactions in a non-adiabatic multichannel catalytic combustion reactor

Stan T. Kolaczkowski [a,*], David J. Worth [b]

[a] *School of Chemical Engineering, University of Bath, Bath BA2 7AY, UK*

[b] *School of Mathematical Sciences, University of Bath, Bath BA2 7AY, UK*

Abstract

The development of a mathematical model to account for channel interactions in a multichannel monolith with square shaped channels is described. As an example of the application of the code, channel interactions are modelled that result from a maldistribution in fuel supply into a catalytic monolith combustor. The response of a metal and a ceramic monolith are compared, demonstrating the advantages of conduction as a method of dissipating heat in the radial direction.

Keywords: Combustion; Channel interactions; Non-adiabatic reactor

1. Introduction

In catalytic combustion applications, where monoliths are used as catalyst support systems, it is possible, under certain conditions, for the neighbouring channels to interact with one another. This may arise (a) unintentionally, e.g. as a result of poor fuel and air mixing, e.g. [1], and subsequent fuel maldistribution into the monolith (see Fig. 1a), or (b) intentionally, e.g. as a result of coating alternate channels with catalyst, e.g. [2]. In both of these examples, both gas and wall temperatures will differ between the neighbouring channels, resulting in heat transfer across the connecting wall and consequential interactions. In case (b), this feature is exploited [2] to reduce surface temperatures in the active channels and also to provide a preheated fuel and air mixture to the next catalytic stage in the combustor. In case (a) however, higher values of inlet fuel concentration may result in the presence of 'hot zones', which, if not dissipated as a result of channel interactions, may cause catalyst/substrate damage. Obviously, in both of these examples, modelling has a role to play, aiding system design.

The modelling of catalytic monolith reactors in a multichannel setting has received little attention compared with a single channel model. Studies over the last six years include the work of: Kolaczkowski et al. [3,4], Worth et al. [5,6] and Cybulski and Moulijn [7]. In general, reactions are modelled in a single channel system based on either a one (1D) or a two dimensional (2D) form of equations. The complexity of incorporating 2D models into a multichannel interacting system would not be practicable, and also difficult to justify for non-circular shaped cells. The rationale of developing a model to account for heat transfer across the wall between neighbouring channels has been described, [3,4], and has since been used

* Corresponding author.

SSDI 0920-5861(95)00149-2

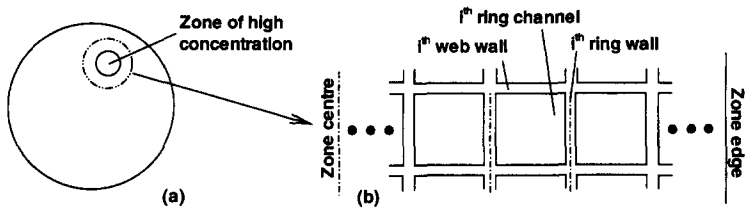

Fig. 1. (a) Indicating a zone of fuel maldistribution on the front face of a circular shaped monolith reactor, (b) modelled zone in a reconfigured structure.

as a building block for the development of more complex models [5,6,8] of reacting systems. In this paper, an example application of the code to simulate a case (a) scenario is illustrated, to demonstrate the type of information that can be obtained from this form of analysis. In the simulation, the fuel is methane and the operating conditions are in a range of interest to developers of gas turbine combustors.

2. The multichannel model

In the monolith reactor the reactants need to be transported to the catalytic sites in order to initiate reactions. The processes of interphase and intraphase mass transfer are therefore important factors. At temperatures between 450 and 800°C, catalytic reactions dominate, whereas above 800°C, homogeneous gas phase reactions are likely to start playing an important role, see Fig. 2.

A fuel maldistribution is assumed at the inlet to a monolith with square shaped channels (Fig. 1a), and the patch of channels around the zone of high concentration is reconfigured to an axisymmetric configuration (see Fig. 3). This simplifying technique was developed in earlier work [3,4] as a way of modelling interactions between neighbouring channels. In the transformation, the overall number of channels in the monolith are preserved, and so is the average number of boundaries from the outside channel to the centre of the monolith. The solid substrate is divided into 'ring' and 'web' elements which are modelled as 'heat sinks', i.e. the heat entering or leaving these sections affects the temperature of that section. Each channel ring contains n_i channels where:

$$n_i = n_d \pi R^2 \left\{ \left(\frac{i}{N_{rg}} \right)^2 - \left(\frac{i-1}{N_{rg}} \right)^2 \right\}, \; i = 1, \cdots, N_{rg}. \tag{1}$$

This allows the mass and energy balances to be solved for a strip of N square channels (Fig. 1b). The behaviour of the original patch of channels is then recovered by rotating the strip.

Axisymmetry means that the web walls on each side of the channels in Fig. 1b have the same temperature, that is, there is no heat flux across these walls. In contrast, each ring wall has a different temperature with temperatures on each surface being different again due to the catalytic reaction. The heat fluxes for channel interaction are illustrated in Fig. 4. In addition to channel interaction, the model includes terms for:

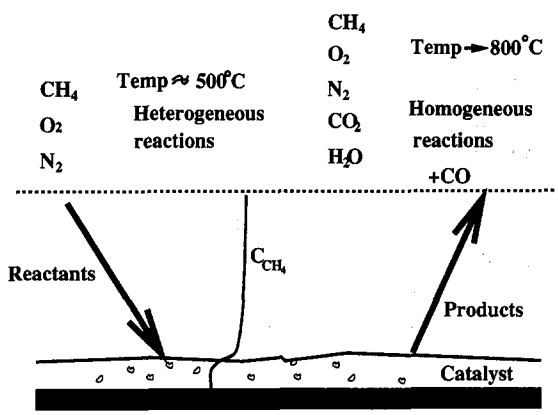

Fig. 2. An outline of the heterogeneous and homogeneous reactions occurring in a monolith reactor.

Fig. 3. Diagram representing the method of reconfiguration to an axisymmetric shape.

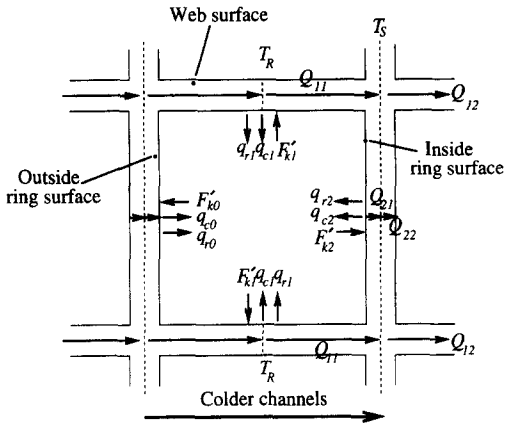

Fig. 4. Channel interaction through the ring walls.

(a) heterogeneous reactions, modelled as a one step process, i.e.

$$CH_4 + 2O_2 \rightarrow CO_2 + 2H_2O\,, \tag{2}$$

(b) homogeneous reactions, modelled as a two step process, i.e.

$$CH_4 + \frac{3}{2}O_2 \rightarrow CO + 2H_2O\,, \tag{3}$$

$$CO + \frac{1}{2}O_2 \rightarrow CO_2\,, \tag{4}$$

with reaction rates taken from [9], (c) heat and mass transfer by convection (using established correlations), (d) solid phase conduction (both in the axial and radial direction), (e) radiation, (f) intraphase diffusion in the washcoat, by solving a boundary value problem, an expression is evaluated for the effectiveness factor η as a function of ϕ, the Thiele modulus, and (g) pressure drop.

The physical properties are described as functions of temperature and composition, e.g. for viscosity, $\mu = A + BT$, where A and B depend on the gas composition.

Mass and energy balances are written for the gas phase, the catalytic surfaces, and the solid walls and yield a complex system of differential-algebraic equations (DAEs) coupled with two point boundary value problems (BVPs) and integral equations (FIE2s). Example equations are:

Gas phase mole balance, e.g.

$$-\frac{dF_{CH_4}}{dx} = r_{CH_4}A_c + F'_{CH_{4_0}} + 2F'_{CH_{4_1}} + F'_{CH_{4_2}}\,, \tag{5}$$

Gas phase energy balance

$$A_c \rho u C_p \frac{dT_B}{dx} = \tag{6}$$
$$-(\Delta H_{CH_4} r_{CHCH_4} + \Delta H_{CO} r_{CO})A_c$$
$$+ q_{c0} + 2q_{c1} + q_{c2}\,,$$

Ring wall surface mole balance, e.g.

$$F'_{CH_{4_2}} = \frac{\sigma}{4} r_{CH_{4_w}}\,, \tag{7}$$

Ring wall surface energy balance, e.g.

$$\frac{\sigma}{4}(\Delta H_{CH_{4_w}} + \Delta H_{CO_w}) r_{CH_{4_w}} = q_{r2} + q_{c2} + Q_{21}, \tag{8}$$

Ring wall energy balance,

$$-A_s \lambda \frac{d^2 T_S}{dx^2} + Q_{21} = Q_{22}\,,$$

with boundary conditions for radiative heat loss from the solid end faces

$$[T_S(0)]^4 - \frac{\lambda}{\epsilon\sigma_E}\frac{dT_S}{dx}\bigg|_{x=0} - T_{bu}^4 = 0$$
$$= [T_S(L)]^4 + \frac{\lambda}{\epsilon\sigma_E}\frac{dT_S}{dx}\bigg|_{x=L} - T_{bd}^4. \tag{9}$$

The heat and mass fluxes (q and F' respectively) are illustrated in Fig. 4.

2.1. Radiation

In the catalytic combustor energy exchange via radiation occurs: within channels, between the channel walls and the black bodies seen through the open ends of the channels, and from the end faces of the substrate walls (see the schematic in Fig. 5 and Eq. 9).

The wall surfaces are assumed diffuse (i.e. the emitted energy is uniform in all directions) and

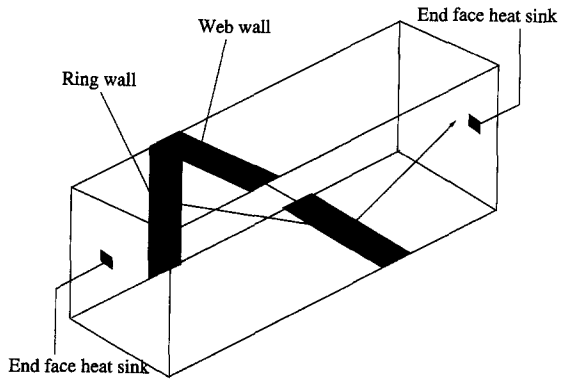

Fig. 5. Radiative transfer in a square channel.

gray (i.e. the emissivity does not depend on the radiation wavelength).

For the square shaped channels a system of integral equations has been developed to model radiative exchange. Approximations to the integral operators are determined which allow the reduction of the integral equation system to a matrix system. This matrix system is solved whenever the radiative heat losses are required in the coupled system of differential and algebraic equations that model the monolith reactor.

2.2. Pressure drop

In general, since pressure drop is small across a monolith reactor, a full momentum balance is not considered necessary provided the effect of temperature on velocity is taken into account. However, in a case where channel interaction is likely to arise, variations in axial temperature profiles between neighbouring channels may cause the mass flow rates into the channels to vary among the channels. This is calculated by evaluating the pressure drop along a channel and ensuring that the overall pressure drop, ΔP, for each of the channels is the same. This is evaluated from:

$$\frac{dP}{dx} = -\frac{4\Phi\hat{\rho}u^2}{d} - \hat{\rho}u\frac{du}{dx}, \tag{10}$$

with

$$u(T,P) = \frac{u_0 T P_0}{T_0 P}, \tag{11}$$

and the friction factor $\Phi = f/2$ (where f is the Fanning friction factor) is evaluated from a correlation. The change in mass flow rates is accomplished by varying the velocities into each channel, u_i, with respect to the average pressure drop ΔP_{av}, using

$$u_i|_{new} = u_i|_{old}\frac{\Delta P_{av}}{\Delta P_i}. \tag{12}$$

The algorithm for this procedure is given in schematic form in Fig. 6. A further adjustment is then made to ensure that the total mass flow rate to the monolith is preserved constant.

3. Solution algorithm

The full model is a differential-algebraic-integral system with first order initial value problems

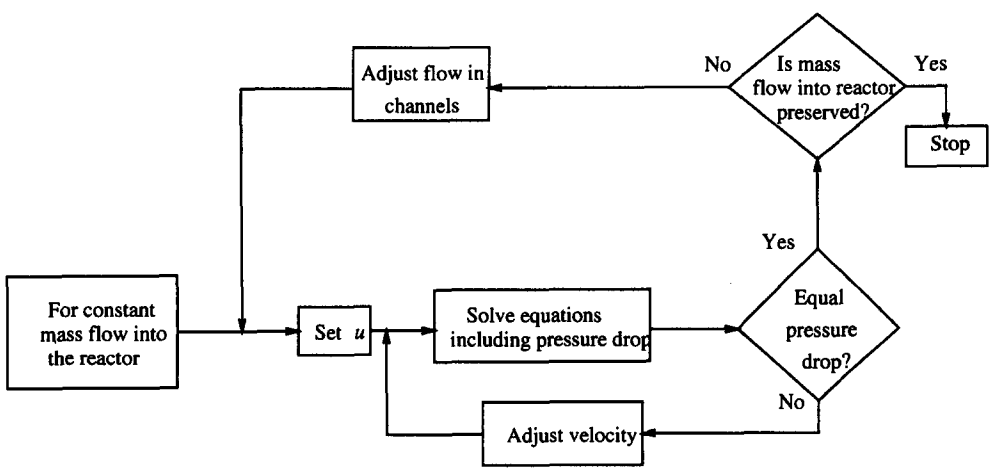

Fig. 6. A schematic of the algorithm for adjusting velocity to equilibrate the pressure drop.

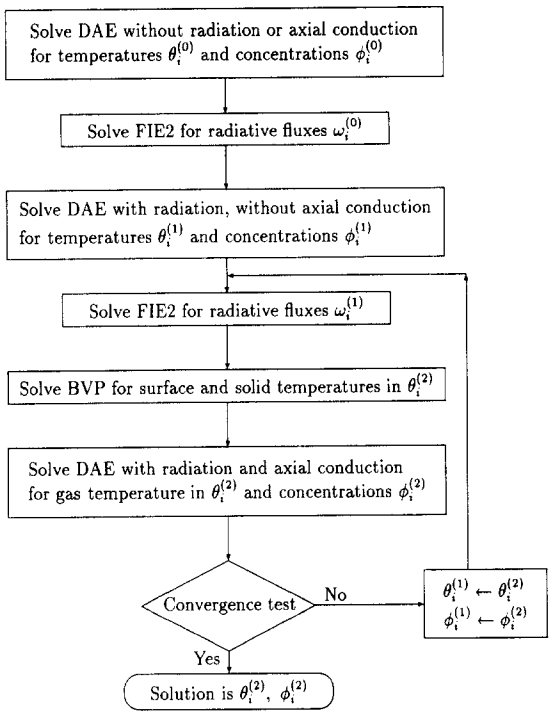

Fig. 7. A simplified flow diagram illustrating the key features of the solution algorithm.

and second order boundary value problems. For a strip of N channels the system is of order $23N+1$ and is coupled to a system of three integral equations per channel. The complexity of the equations and the coupling in the system make it necessary to use numerical techniques to solve this large system of equations. The solution method divides the problem into three parts, and is described using a flow chart in Fig. 7. Firstly, solid phase conduction and radiation are neglected and the equations which now form a differential-algebraic system (DAE) are solved. (See [10] for an introduction to DAEs and their numerical solution.) Using the solution found, the radiation fluxes are then calculated utilising the approximations of the integral equations. In order to keep the radiation effect on temperature the DAEs are solved again including radiation. A further solution of the radiation equations is carried out before axial conduction is included by solving the boundary value problem. The next solution of the DAE now shows the effect of radiation and axial conduction and if necessary the process is iterated to find a converged solution.

Table 1
Initial and physical conditions for simulations in Fig. 8

Inlet gas temp	811 K
Inlet gas pressure	9.92×10^5 Pa
Inlet gas velocity	25.24 m s^{-1}
Upstream blackbody temp	811 K
Downstream blackbody temp	567.7 K
Air to fuel ratio (by mass)	291
Channel hydraulic diameter	9.33×10^{-4} m
Solid wall thickness	1.5×10^{-4} m
Monolith length	0.0508 m
Diameter of modelled zone	0.02166 m

4. Results

Example results for the case of simulating an inlet fuel maldistribution (see Fig. 1a) for the conditions described in Table 1 are given in Fig. 8 and Fig. 9. The responses of a metal and a ceramic monolith are compared, and it is clear from the radial plots (Fig. 8) that channels interact, transferring energy between channels and increasing reaction rates. It is also noticeable that the metal monolith transfers heat from hot channels to cooler channels more readily than the ceramic one. When radiation is considered, the inlet and outlet wall temperatures decrease due to the heat losses from the ends of the monolith. This is clear from the axial plots in Fig. 9 where it is also apparent that radiation only appears to affect the channel ends and not the central regions. This is because, for the reactor simulated, the energy exchange is mainly with the opposite and adjacent wall surfaces which are at similar temperatures.

The simulations were performed for a proprietary palladium based catalyst system with a mean washcoat thickness of 50 μm and a mean pore diameter of 100Å. Because of commercial constraints it is not possible to provide more detailed information on the catalyst or the form of the kinetic rate expression used.

5. Concluding remarks

Mathematical modelling of monolith reactors provides valuable information about the physico-

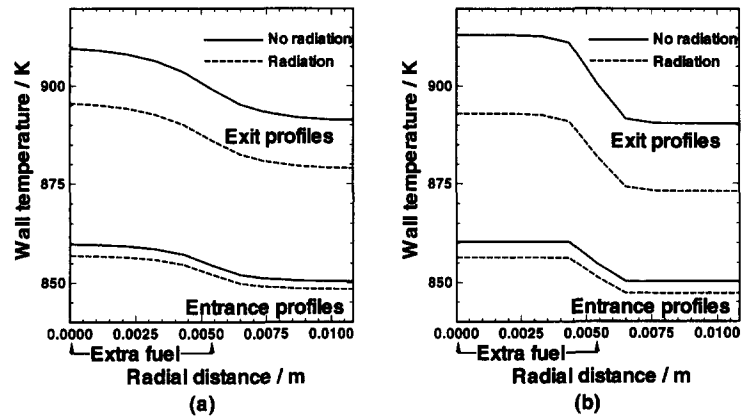

Fig. 8. The wall temperatures for (a) a metal and (b) a ceramic monolith, at the monolith entrance and exit for an inlet fuel maldistribution where the centre 10 channels in the zone have an inlet F_{CH_4}, 30% higher than the other channels which are operating with AFR = 291.

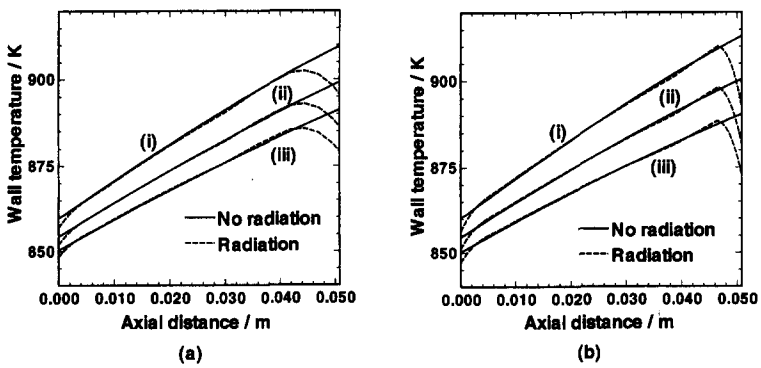

Fig. 9. The wall temperature vs. the axial distance for (a) a metal and (b) a ceramic monolith. Fuel maldistribution as in Fig. 8, where (i) the wall at the centre of the high concentration zone, (ii) the wall between the high concentration and the low concentration zone, (iii) the wall at the boundary of the modelled zone.

chemical processes taking place and how these affect the performance of the reactor. In the example simulation of a hot spot, the differences in the performance of a metal versus a ceramic monolith are apparent. By using a model of this type, quantitative data can be obtained (e.g. on variations in wall temperatures), which will aid system design. However, the quality of mathematical models is highly dependent on the basis of the assumptions made, numerical techniques employed and the validity of the physical and chemical parameters (e.g. kinetic expressions, physical properties) used in them. It is important that modellers should work in parallel and together with experimentalists to ensure that a holistic approach to system design is followed.

The simulations presented in this paper illustrate how modelling techniques may be applied to support experimental trials. Further work is necessary, however, to validate the model developed with experimental data from non-adiabatic experiments.

6. Nomenclature

A	coefficient in viscosity correlation
A_c	channel cross-sectional area (m^2)
A_s	solid wall cross-sectional area (m^2)
AFR	air/fuel ratio by mass
B	coefficient in viscosity correlation

C_p	gas heat capacity (J mol^{-1} K^{-1})
F'	molar flux (mol m^{-1} s^{-1})
F_{CH_4}	CH_4 molar flow rate (mol s^{-1})
L	monolith length (m)
N	number of channels in simulation, i.e. number of rings simulated
N_{rg}	number of rings in reconfigured monolith
n_d	monolith cell density (cells m^{-2})
n_i	number of channels in ith ring
P	gas pressure (Pa)
Q_{11}, Q_{12}	solid phase heat flux in web wall (Fig. 4) (W m^{-1})
Q_{21}, Q_{22}	solid phase heat flux in inside ring wall (Fig. 4) (W m^{-1})
q	heat flux into gas phase (Fig. 4) (W m^{-1})
R	radius of monolith (m)
r_{CH_4}	reaction rate for Eq. 3 (mol m^{-3} s^{-1})
r_{CO}	reaction rate for Eq. 4 (mol m^{-3} s^{-1})
$r_{CH_{4w}}$	reaction rate for Eq. 2 (mol m^{-2} s^{-1})
T	temperature (K)
T_{bu}	upstream blackbody temp (K)
T_{bd}	downstream blackbody temp (K)
u	gas velocity (m s^{-1})
x	axial distance (m)
ΔH_{CH_4}	heat of reaction for Eq. 3 (J mol^{-1})
ΔH_{CO}	heat of reaction for Eq. 4 (J mol^{-1})
$\Delta H_{CO_{4w}}$	heat of reaction for Eq. 2 at wall surface conditions (J mol^{-1})
ΔH_{COw}	heat of reaction for Eq. 4 at wall surface conditions (J mol^{-1})
ΔP	pressure drop (Pa)
ϵ	surface emissivity
η	effectiveness factor
$\theta_i^{(0)}, \theta_i^{(1)}, \theta_i^{(2)}$	nondimensional temperatures in Fig. 7
λ	solid wall thermal conductivity (W m^{-1} K^{-1})
μ	gas viscosity (Pa s)
ρ	molar density of gas (mol m^{-3})
$\hat{\rho}$	mass density of gas (kg m^{-3})
σ	channel perimeter (m)
σ_E	Stefan-Boltzmann constant (W m^{-2} K^{-4})
Φ	friction factor
ϕ	Thiele modulus
$\phi_i^{(0)}, \phi_i^{(1)}, \phi_i^{(2)}$	nondimensional concentrations in Fig. 7

Subscripts

av	average value
c	convective flux
k	species (Fig. 4)
r	radiative flux
W	wall surface phase
0	outside ring surface (Fig. 4)
2	inside ring surface (Fig. 4)
B	gas phase
i	ith channel
R	referring to the web wall
S	referring to the ring wall
0	inlet value
1	web surface (Fig. 4)

Acknowledgements

This paper reports some of the work on developing mathematical models of catalytic combustion systems for gas turbines which is funded under the DTI/SERC LINK scheme into New Catalysts and Catalytic Processes. (Research grant no. GR/H00734)

References

[1] W.S. Blazowski and D.E. Walsh, Combust. Sci. Technol., 10 (1975) 233.

[2] R.A. Dalla Betta, N. Ezawa, K. Tsurumi, J.C. Schlatter and S.G. Nickolas, US Patent 5183401, 1993.
[3] S.T. Kolaczkowski, P. Crumpton and A. Spence, Chem. Eng. Sci., 43 (1988) 227.
[4] S.T. Kolaczkowski, P. Crumpton, R.P.J. Lee and A. Spence, Chem. Eng. J., 42 (1989) 167.
[5] D.J. Worth, S.T. Kolaczkowski and A. Spence, Chem. Eng. Res. Design, 71 (1993) 331.
[6] D.J. Worth, Ph.D. Thesis, School of Mathematical Sciences, University of Bath, 1994.
[7] A. Cybulski and J.A. Moulijn, Chem. Eng. Sci., 49 (1994) 19.
[8] A. Spence, D.J. Worth, S.T. Kolaczkowski and P.I. Crumpton, Computers Chem. Eng., 17 (1993) 1057.
[9] F.L. Dryer, Ph.D. Thesis, Department of Aerospace and Mechanical Sciences, Princeton University, 1972.
[10] K.E. Brenan, S.L. Campbell and L.R. Petzold, Numerical Solution of Initial-Value Problems in Differential-Algebraic Equations, North Holland, Amsterdam, 1989.